Design and Implementation of Non-prehensile Manipulation Strategies

Pooja Bhat, Matthias Nieuwenhuisen[a] and Dirk Schulz[b]
Fraunhofer Institute for Communication, Information Processing and Ergonomics FKIE, Wachtberg, Germany

Keywords: Non-prehensile Manipulation, Force-torque Control, Compliant Manipulation.

Abstract: Grasping of objects is not always feasible for robot manipulators, e.g., due to their geometric properties. Non-prehensile manipulation strategies can enable manipulators to successfully move these objects around. We discuss strategies for non-prehensile manipulation and focus on the investigation of such manipulation strategies based on open- and closed-loop control based on force torque measurements. The design of grippers for moving objects is also an important factor that is evaluated. The strategies are implemented and evaluated in simulation and on a KUKA LWR4+ manipulator arm.

1 INTRODUCTION

Robotic manipulation tasks are often defined by grasping or picking an object from a surface or a box and place it on another place. But in everyday situations, we humans often use different strategies to move objects around, e.g., pushing or sliding. In fact, the ability to skillfully perform non-prehensile manipulation tasks contributes greatly to manipulative dexterity of humans. Humans tend to exploit finger configurations with natural haptic and force feedback while handling a diverse set of objects.

These non-prehensile manipulation strategies can help a robot manipulator to move around objects that are too heavy, too small, or to flat to be grasped with a specific gripper. Figure 1 shows the handling of different types of objects that are not easy to grasp due to their geometric properties.

In addition to pushing objects from the side in some cases applying a perpendicular force on an object to move it around is better suited, for instance if the object is very flat and lightweight, e.g., a sheet of paper.

Humans exhibit advanced prediction capabilities which enable estimation of the best action to be taken to achieve the desired state, which means inverse model is assimilated by visual analysis, and/or is learnt during execution based on action-effect paradigm. Also, humans are capable of transferring the learnt behavior to novel objects with different physical properties (Stüber et al., 2022). However,

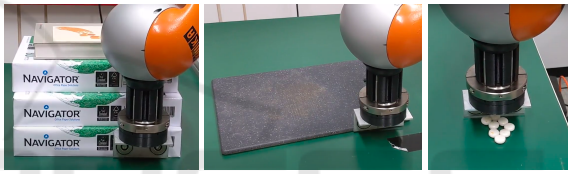

Figure 1: Non-prehensile manipulation like pushing allows robots to handle objects that are hard to grasp, e.g., heavy, flat, or small objects.

pushing involves various uncertainties that robots cannot predict which prevent them from delivering similar pushing behavior. The main cause of this uncertainty is the inadequate knowledge on frictional forces which play significant role in pushing (Zhou et al., 2016). Also, the pushing dynamics is highly non-linear (Yu et al., 2016). While various proposed approaches have delivered accurate forward models for push-effect prediction, generalisation of the models to novel objects has still remained a challenge (Stüber et al., 2018; Stüber et al., 2022).

Planning and controlling of various non-prehensile motions such as pushing, rolling, throwing, juggling have been explored in the literature (Serra, 2016; Ryu et al., 2013; Lynch and Murphey, 2003). The survey in (Ruggiero et al., 2018) summarizes the advancement in planning and control of all these motions and provides an extensive literature review. It further concludes that the growth in the field of non-prehensile manipulation is relatively low and human-inspired control strategies could provide a potential solution to complex non-prehensile manipulation tasks.

A comprehensive literature review is provided on

[a] https://orcid.org/0000-0002-3706-592X
[b] https://orcid.org/0000-0002-6240-9181

Bhat, P., Nieuwenhuisen, M. and Schulz, D.
Design and Implementation of Non-prehensile Manipulation Strategies.
DOI: 10.5220/0011320700003271
In *Proceedings of the 19th International Conference on Informatics in Control, Automation and Robotics (ICINCO 2022)*, pages 67-78
ISBN: 978-989-758-585-2; ISSN: 2184-2809

push manipulation in (Stüber et al., 2022), considering it effective in various scenarios, for instance, with uncertainty in the environment, and with need for pre-grasp manipulation. In general, push manipulation is used to maneuver objects from initial state to goal state when the grasping of object is not feasible, e.g., due to object geometry. In addition, pushing is largely used for pre-grasping to facilitate grasping of the object, e.g., to create space in presence of clutter.

Directed standalone pushing is used in the literature vastly by mobile robots that are not equipped with any manipulators. In (Krivic and Piater, 2018; Krivic et al., 2016), objects are pushed with a single contact towards a defined goal while learning the properties of the object on the fly by observing their behavior when pushed. In (Krivic et al., 2016), the target object is expected to remain in a defined corridor, a region that is free of obstacles. The system has to autonomously relocate when needed to execute pushing towards the defined goal. These works mainly relax the assumption on knowing about the key geometric properties of the objects to generalize for novel objects, but apply basic single contact pushing due to the lack of manipulators. In (Li and Payandeh, 2007), two-agent point contact push is proposed to allow more than one contact point using two agents to push the target. This facilitates manipulation of non-polygonal parts reducing position uncertainties.

Robot manipulators use pushing as an alternative to grasping in various cases. In (Zito et al., 2012), two level rapidly exploring random tree (RRT) planners are designed, of which a global planner explores the space of possible pushed object configurations and a local push planner uses predictive models of pushing interactions, to plan push sequences. A learning based technique leverages differentiable physics simulator to learn mechanical properties of the unknown object to push it from initial to goal configuration in (Song and Boularias, 2020). The method computes gradient distance between predicted and actual poses and uses the gradient to identify the mechanical properties.

When an object is located in a clutter, pushing is performed around the target object to achieve graspablity. While in (Dogar and Srinivasa, 2010), the target object is pushed away and grasped, in (Zeng et al., 2018; Dogar and Srinivasa, 2011; Cosgun et al., 2011), the surrounding objects are pushed. The surrounding objects are pushed to create space to place target object on a cluttered surface in (Cosgun et al., 2011). It is important to note that in push-grasp literature, the planning is mostly in the higher level to generate a sequence of pushes that is required enable the manipulation of target object. As the goal state of the surrounding objects are the not the primary concern in these cases, controlled pushes are not applied on the objects.

The application of pushing as pre-grasp manipulation is not exclusive for cluttered environments, but is integrated in the manipulation strategies in a handful of grasp planners. A human-inspired grasping framework is proposed in (Sarantopoulos and Doulgeri, 2018) to grasp domestic flat objects, which uses pushing/sliding to bring the object to the edge of the table surface to eventually grasp it with one of the proposed strategies. In (Eppner and Brock, 2015), the aim is to utilize environmental constraints to grasp the objects, and the objects are pushed to achieve configuration such that they can be grasped with the support of external contacts. However, the pushes used in these approaches are constrained by position and geometric properties of the objects. For example, the strategy proposed in (Sarantopoulos and Doulgeri, 2018) cannot slide the objects that are far from the edge of the table surface. In (Omrčen et al., 2009), a learning-based approach is proposed to enable pushing of target object to new location from where it can be grasped easily. The idea is to allow a robot learn general pushing rule defining the relationship between the direction of push and the resulting object motion for a set of objects.

Although pushing is widely used to manipulate objects, it suffers from prediction and state uncertainties (Stüber et al., 2022). Planning and control of pushing motion is hence challenging when a hard goal constraint is imposed as inverse model is not available to predict the action to be taken to achieve the desirable state. The problem becomes more complex with varying geometric shapes and sizes of the target object. Majority of the approaches investigated in (Stüber et al., 2022) assume that the geometric properties of the target objects to be known. This assumption does not bridge the gap between the dexterity of humans and robots in non-prehensile manipulation.

2 SYSTEM DESIGN

The analysis provided in the previous section highlights the dissimilarities in the human and robot push manipulation which mainly includes the difference in the push contact configuration and lack of knowledge on the push-effects due to unavailable object dynamics. In this work, the important constituents of push manipulation are recognised and designed to provide a human-inspired solution. The aim is to deliver a design solution that provides push manipulation of a vast set of objects with varying geometric properties.

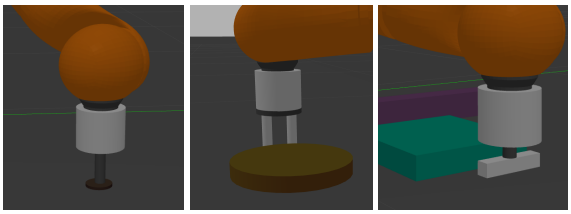

Figure 2: Endeffector configurations for pushing. Left: Single point contact. Center: Multi-point contact. Right: Line contact.

2.1 Gripper Configurations

Humans tend to relax high-level control by exploiting available finger configurations while handling a diverse set of objects. However, robots mostly use a single point contact for push applications relying on complex control for task execution. While single point contact is easy to establish with a simple rigid finger or no gripper, a dexterous gripper attachment providing features of human hand is not a cost effective solution. To compensate for the trade-off, in this work, simple human-inspired gripper configurations are proposed: single-point contact, multi-point contacts, line contact.

Each of these grippers are designed considering hand positioning tendency in humans with varying geometric properties of the objects. With a dexterous gripper possessing at least two single-joint fingers, all the configurations can be generated with the same gripper. However, in this work, different gripper attachments are designed. Figure 2 depicts the three realized gripper configurations.

Single Point Contact. Gripper configuration providing single point contact allows the manipulator to apply force on the object at a single point. In the push manipulation literature, single point contact is usually established such that the applied pushing force lies horizontal to the support plane while gravity acts along the vertical direction. However, applying vertical force on the object constrains the sliding of the object due to high pushing force. With this configuration, small objects such as a bottle cap can be manipulated.

Multi-point Contact. A two-point contact is shown to deliver a more stable push compared to a single point contact in (Lynch, 1996). This configuration can be useful when achieving more stable control over the objects is required, for instance, when they are relatively flat and deformable, e.g. files, cards. This gripper configuration also finds application in manipulating taller objects with convex/concave surfaces.

Line Contact. When objects are too heavy and/or big, prehensile manipulation can be restricted by gripper design. When the target object is a heavy book or a box, pushing it from the side while almost wrapping one or more fingers around the object can be an alternate solution. Also, humans use such pushing strategy to handle odd shaped objects or multiple objects at once.

With the proposed human-inspired design of gripper configurations, this work aims to handle a diverse set of objects with non-prehensile approach using simple control strategies.

2.2 Control

Humans depend on their natural haptic and force feedback to control contact forces. Similarly, the contact force between a robot and its environment should often be monitored to ensure successful execution of tasks which requires the robot to interact with its environment. The control interfaces that enable such *compliant* behavior are discussed in this section.

Further, various control strategies designed to compensate for the lack of dexterity and haptic feedback in human hands are explained. The control strategies coupled with gripper design aims to prevent undesirable effects in the motion of the target objects as opposed to previously discussed learning based approaches that learn to predict the effects of pushes for push manipulation.

When a robot has to push the target object, a perpendicular external force is exerted on the support surface even before any force is applied on the object. The force between a gripper and a surface has to avoid any damage to the robot and its environment. Further, the applied force by a robot to push the target object plays an important role in the execution of push manipulation. Hence, it is necessary to control push force to avoid sliding of the objects away from robot gripper. This section discusses different robot control modes that can be used to obtain desirable interaction.

Open-loop Motion Control with Force-torque Sensor. To use pure motion control for the tasks involving contact between a robot manipulator and the environment, an accurate model of the environment is required (Siciliano et al., 2000). As a precise model of the environment is difficult to obtain, pure motion control easily fails to handle such tasks. If the accurate position of the table with respect to robot is not known, the robot fails to establish contact with the table. In worst case, if the table resists the robot from reaching its commanded position, the robot may damage the table and/or itself.

Hence, it is important to detect contact between the robot and the environment. To achieve this, a force/torque sensor can be mounted on the manipulator to sense the physical interactions (Alex Owen-Hill, 2021).

Impedance Control. Impedance control is a widely used method to obtain compliant behavior in robots (Schindlbeck and Haddadin, 2015; Ott et al., 2010). It defines the change in endpoint motion as a function of disturbance forces. It demands robots to deliver a definite mass, spring, and damper properties.

The goal of impedance control is to achieve the behavior

$$M\ddot{x} + D\dot{x} + Kx = F_{external} \tag{1}$$

where M, D and K are positive virtual mass, damping and stiffness matrices, $x \in \mathbb{R}^n$ is the task-space configuration and $F_{external}$ is the applied external force and $(x, \dot{x})$ is the current state.

The impedance controller senses the endpoint motion $x(t)$ and maps the change in endpoint motion to appropriate end-effector force $-F_{external}$ by commanding joint torques using an inverse dynamics model. To get a more precise interaction force $-F_{external}$, a force-torque sensor providing a feedback term can be added at the end-effector (Lynch and Park, 2017). In addition to impedance control that is realised via software, compliance can also be achieved with passive impedance control by manually adjusting mechanical impedance of the robot with flexible joints and/or links (Vukcevic, 2020). In addition, a compliant mechanical device can be interposed between robot end-effector and environment to ensure a compliant behavior with passive impedance control. Both active and passive impedance control can also be combined to achieve an effective compliant behavior (Schindlbeck and Haddadin, 2015).

Admittance Control. When executing non-prehensile tasks such as pushing, the robot should offer a compliant behavior to provide a controlled pushing force in the desired directions. To induce compliant behavior, an external admittance control loop can be provided to the motion-controlled robot (Al-Jarrah and Zheng, 1998). Admittance control maps external force to end-effector acceleration. The external force applied is measured using a load cell or a force-torque sensor (Lynch and Park, 2017).

The approach is to calculate the desired end-effector acceleration

$$\ddot{x}_{desired} = M^{-1}(F_{external} - D\dot{x} - Kx) \tag{2}$$

where M, D and K are positive virtual mass, damping and stiffness matrices, $x \in \mathbb{R}^n$ is the task-space configuration and $F_{external}$ is the applied external force and $(x, \dot{x})$ is the current state. The commanded joint forces and joint torques τ_{cmd} can be calculated using inverse dynamics (Lynch and Park, 2017).

2.3 Control Strategies

Compliant control strategies are needed along with well-designed grippers to provide a robust control to perform better in unideal situations. The underlying objective is to not lose contact with the pushed object. While a visual feedback can also be utilised to locate the pushed objects and re-establish contact if the objects slide away, in this case, only force feedback is taken into account to monitor physical interactions.

To maintain contact with the target object while applying a suitable force on the target object to induce desirable motion, a 1-DOF admittance control policy is used to map the force/torque measured to push velocities such that,

$$D\ddot{x} = F_{external} \tag{3}$$

from equation 2.

Alignment of Gripper along Object Surface. When a robot gripper is not well aligned along the surface of the target object, the contact between gripper and the target object can be broken easily. Consider the example gripper-object configuration from top-view shown in figure 3 (left) where "O" is a target object and "G" is a line contact gripper. The line gripper here is not perfectly aligned along the surface of the object. When the robot continues to push the object in this configuration, the object tends to rotate and eventually loses contact with the gripper as shown in figure 3 (center). Hence, it is necessary to align the gripper along the object surface to avoid the undesirable rotation of object. The torque produced at the center of the gripper along perpendicular direction due to the existing force between the object and the corner of the gripper can be mapped to a linear velocity along the surface of the gripper given by,

$$v_y = -k_y \tau_z \tag{4}$$

where v_y is the velocity along the surface of the object, τ_z is a non-zero torque at the center of the gripper about z-axis and k_y is the proportional gain. This allows gripper to move to the center of the object and achieve a desirable configuration as shown in figure 3 (right) where torque $\tau_z = 0$. However, it is necessary to choose a suitable proportional gain to obtain a smooth alignment without oscillations.

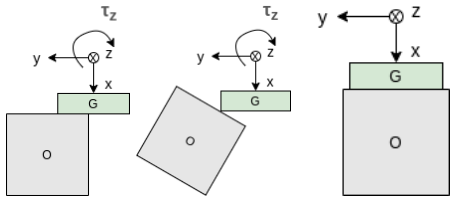

Figure 3: Effects of alignment of an endeffector (G) with an object (O) based on torque (τ_z).

Regulation of Push Velocity during Alignment. To allow smooth pushing motion, it is necessary to control push velocity such that the velocity along push direction, for example, v_x in figure 3 is maximum when alignment velocity $v_y = 0$ which means the torque $\tau_z = 0$ and is minimum when the torque and alignment velocities are high. The behavior can be achieved by mapping the torque τ_z to push velocity v_x.

Emulation of Curved Gripper. Humans tend to form a curved configuration, especially when small multiple objects are to be pushed, to keep the objects integrated. This could be resembled by a curved gripper design. An alternate solution could be provided to induce the feature of curved gripper configuration in a line gripper by inducing timed oscillations into it as shown in figure 4. The cyclic angular motions are commanded here about z-axis to produce oscillations at a definite frequency rate. This enforces pushing of objects from either sides of the gripper to the center to keep objects integrated. Additionally, the torque induced about z-axis from the target object at the corner or at the off-center of the gripper can be mapped into angular velocity providing a closed loop control given by,

$$\omega_z = k_z \tau_z \tag{5}$$

where ω_z is the angular velocity about z-axis, τ_z the measured torque, and k_z is a proportional gain. In this case, oscillations do not occur at constant rate but, angular motions depend on the torque generated by the virtue of the position of the target object. When the object/s are at the center of the gripper, no angular motions are generated. This case demonstrates the role played by the design of gripper in simplification of control strategy. If a curved gripper is used over a simple line gripper, the design of the gripper compensates for the control. A simple gripper however relies more on the control strategy.

2.4 Software Architecture

In order to provide a suitable software design pattern for the execution of actions in a pre-defined sequence, a state machine is implemented such that each state

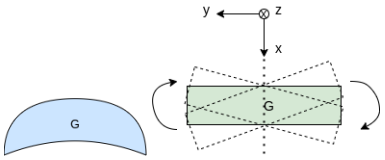

Figure 4: Comparison of curved gripper and oscillated line gripper configurations.

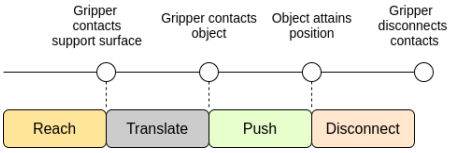

Figure 5: An action sequence for a push manipulation task.

in the state machine corresponds to an atomic action that can be invoked from the action sequence. The action states command velocities to actuate the desired actions and end of each action is marked by a subgoal encoded into the states. Each state is independent of each other, providing a flexible arrangement of actions in the action sequence. Our actions are: *Reach:* In this phase the robot end-effector moves towards the target object and lands behind the object surface in the pushing direction on the support surface. The goal is to form contact with support surface and not with the object surface. The phase ends when robot forms contact with the support plane. *Translate:* The robot is expected to form contact with object in this phase. It translates towards the object while in contact with the support plane. The end of the phase is signified by the contact event between robot gripper and object surface. At the end of this phase, the gripper is in contact with both object and support plane. *Push:* While pushing is a an atomic action by itself, the action can be decomposed and organised in a way to avoid continuous pushing for more flexibility. For instance, the robot can be commanded additional actions to *raise* and *reorient* to disconnect and reconnect contacts to provide more possible actions. Such discretisation allows robot to change the orientations and directions of push with no constraint of pushing in a continuous trajectory. When the object reaches pre-defined goal location, the phase is ended. *Disconnect:* All the contacts can be detached once the goal is reached and the robot can return to its "home" position. The *reorient* and *raise* actions can also be utilised for the purpose.

Figure 5 shows an action sequence with four action-phases with different atomic actions.

3 EVALUATION

We conducted experiments both, in simulation and on a 7-DoF KUKA LWR 4+ robot arm.

The real robot arm provides torque measurements for each of its joints and an estimated external Cartesian force and Cartesian torque acting on the endeffector. However, the torque estimate is not reliable, as in our scenarios forces applied to different positions of the endeffector yield a large torque at the first robot joint due to the long lever. Thus, as our endeffector axis is perpendicular to the surface, we use the torque measured at the endeffector joint in this work along with the estimated external force to obtain a better estimate.

An interface between external computer and KUKA Robot Controller (KRC) can be established using Fast Research Interface (FRI) library provided by KUKA. The FRI library can be used to command robot in joint position, joint impedance and cartesian impedance control modes. A library extending a higher level interface over the original FRI communication protocol is provided by the Stanford Artificial Intelligence Laboratory.

In this work, Robot Operating System (ROS) interface developed by the Research Center E. Piaggio[1] is used to provide realization in a standard, agile control framework. Also, the ROS interface enables necessary tools for robot simulation and visualisation. The ROS package for KUKA LWR [1] provides final interfaces with KUKA FRI, Stanford FRI library and also includes Gazebo simulation plugin.

3.1 Pushing with KUKA LWR4+ Robot

The experiments were conducted with a stack of paper bundles and a book, and a cutting board which is comparatively lighter, depicted in figure 1. In these cases, a line gripper can be seen pushing the objects from a side surface. As the gripper is not aligned at the center of the surface of the objects, the measured torque (about z-axis in this case) is then mapped to the linear velocity along the surface of the object (velocity in x-axis) to provide a better alignment. The line gripper has a push contact with a board with a stack of objects at one of its corners. If the contact is established perfectly at the center of the gripper, ideally, no torque is produced. However, if unaligned, a high torque can be observed depending on the distance between the point of contact and the center of the gripper and on the mass of the object/s.

The commanded velocities and the measured torque in push manipulation executed with the above

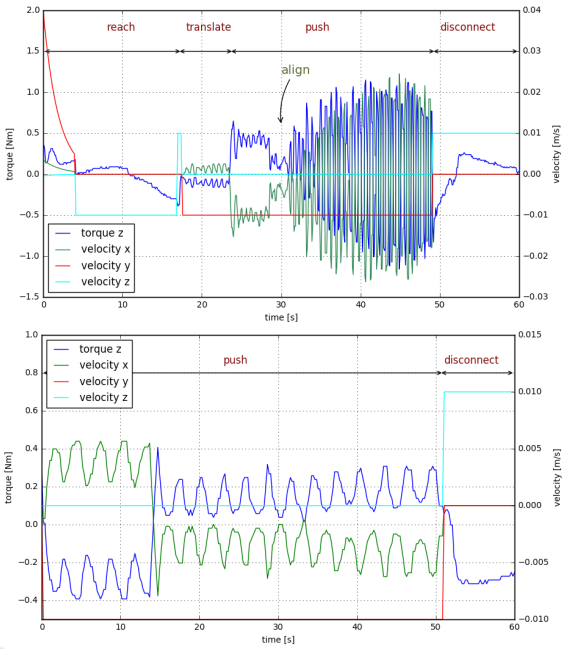

Figure 6: Torque measurements from push manipulation of a set of objects with different geometric properties and orientations in a real world scenario (depicted in figure 1). Top: Stack of paper bundles. Bottom: Cutting board.

mentioned cases are shown in figure 6. As in all the considered cases, the torque produced has to definitely reflect in the torque measurements in z-axis, it is taken into consideration for evaluation. The torque measurement from the push manipulation of the stack of paper bundle and a book is shown in the top graph. In the *reach* phase, the robot moves down towards the object and touches the support surface. The velocity is commanded in z-axis to achieve this motion. Ideally, the torque should be zero, as there is no force acting on the gripper. However, some torque can be observed in the reach phase due to noise in the sensor readings. A small upward movement is commanded during experiment after the robot makes contact with the support surface so as to avoid scratching of the surface by the gripper. A peak in the velocity in z-axis signifies this movement.

An online sensor calibration is performed after the contact with the surface. In the *translate* phase, a small torque can be observed. A sharp increase in the torque value is due to the contact established with the target object. The torque is mapped to linear velocity which causes the velocity in x-axis to exhibit a negative correlation with the torque values. At the point of alignment, at approximately 30 seconds, the torque and velocity drop indicating a good alignment with the object. Although line gripper is aligned at the center, the oscillations can be observed as the system is under-damped. The torque values drop again

[1] https://github.com/CentroEPiaggio/kuka-lwr

when the contact is disconnected by moving the gripper away from the object and the support surface.

When a push manipulation is executed with the similar order of actions for a board which is comparatively much lighter than the stack of paper bundle, a very small torque (maximum 0.2 Nm) is measured. The alignment velocity in x-axis is also consequently small, hence producing an average alignment during pushing. Although robot managed to align approximately at the center of the board during experiment, it is hard to interpret the point of occurrence of alignment unlike in the case of paper bundle stack.

When line gripper makes a contact at the corner of the board, the contact does not lie exactly at the center of the gripper, which induces considerably high torque due to the high mass of a paper bundle and a book stacked on the board. This causes the controller to react and produce an alignment velocity which causes motion of the robot to align to the center. In this case, the board slid slightly to the other off-center when the robot tried to align causing a sharp change in the direction of torque at around 15 seconds. The board then remained in the same contact configuration which is indicated by a non-zero torque in the graph. The *push* phase is ended when the robot disconnects from the object and the support surface.

3.2 Pushing in Simulation

We use the gazebo plugin provided in the KUKA LWR ROS package to control the robot in simulation. As the joint torque measurements in simulation are not accurate as the commanded torques are not taken into account while computing estimated external torques, we employ a force-torque-sensor plugin to obtain wrench measurements at the endeffector, in contrast to the real robot setup.

The experiments conducted to evaluate the performance of the force/torque sensor plugin in simulation is similar to that of the real robot platform. As in the case of real robot, the push manipulation is executed on various objects that differ in size, shape and mass. In addition, the corner-to-surface contact configuration between the gripper and the target object is also considered for the experimentation.

The simulated objects to push are a) a heavy block (2kg), b) a slab (200g), c) a disc (100g), and d) a block (1kg). In the first two cases (a and b) the gripper establishes an even contact on a side surface of the target object. Even though the objects heavy block and slabs are comparable in shape, they vary in mass. The line gripper establishes a centered contact with the curved curved surface of the disc (c). The block (d) is aproached fat one of its corners. The results are depicted in figure 7.

The measured force/torque values are in the sensor co-ordinate frame in simulation. Hence, the torque due to push manipulation in the experiments in reflected in torque about x-axis. For the heavy block (a), in the *reach* phase the robot moves down with velocity commanded in the z direction. In this phase, no external force is acting on the robot end-effector and the measured torque is zero, thus providing an ideal measurement as opposed to real robot sensors which usually possess some noise. In the *translate* phase, a small torque can be observed due to contact with the support surface. The sudden increase in torque signifies the established contact with the target object approximately at 36 seconds. The robot continues to push the object while aligning along the surface of the object which is represented by the oscillating torque and velocity values in x direction.

When the slab (b) with comparably low mass is pushed, a very small torque is induced. The *reach* and *translate* phases are however comparable to the corresponding phases in the case of heavy block in terms of torque measurements. The robot in this case is able to align along the surface but does not behave as good as with a heavy object. The results from these two experiments are comparable to the first two experiments on a real robot with the stack of paper bundle and a board. The push manipulation of the light weighted disc (c) also exhibits similar behavior as with the slab. The curved surface however adds an additional challenge in pushing which causes the line contact gripper to barely maintain a contact with the disc. During pushing, the disc moves off-center and eventually loses contact with the gripper at approximately 45 seconds.

In the configuration where the contact is established by the gripper at a corner of the block (d), the torque values are considerably higher than zero in the *translate* phase as the corner is not perfectly at the center. The motion induced by alignment velocity in x direction causes the object to slide along the surface of the gripper in a “to and fro” fashion. This behavior is captured in a roughly periodic curve.

3.3 Gripper Configurations

The three different gripper configuration designs described in this work are evaluated on a different set of objects. Each gripper configuration is designed with a purpose so as to collectively provide pushing of objects with various geometric properties. In the conducted experiments, the objects are chosen for each gripper with an aim to corroborate their relevance and identify their limitations.

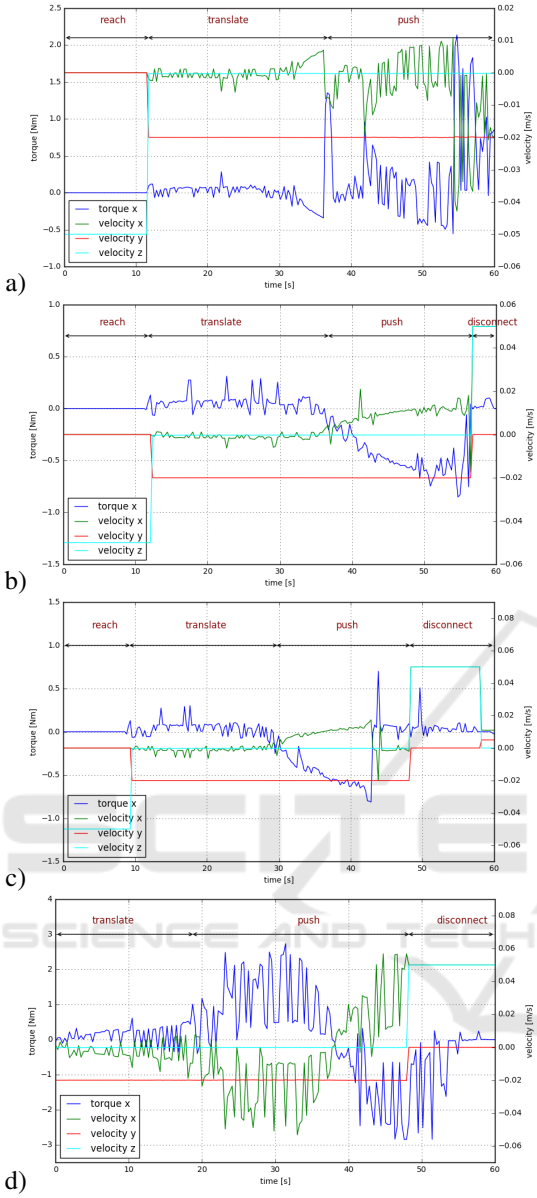

Figure 7: Torque measurements from push manipulation in simulation environment. a) Heavy block. b) Slab. c) Disc. d) Block.

Single Point Configuration. To set up a single point gripper configuration, a sponge block is attached to the manipulator as shown in figure 8. This also serves as a source for passive compliance when a contact is established with the environment. Although the sponge attachment mostly delivers a higher surface contact for a "point" contact, the point contact is only relative to the geometry of the target object.

In this experiment, the single point contact is used to manipulate a set of objects possessing various geometric properties. A set of flat and deformable (tissue), flat and wide (board), small (box), tall and light (cylinder), flat and heavy (paper bundle) objects are manipulated as shown in figure 8. The robot is expected to establish a contact on the top surface of the object and push it to a defined location while clamping the object against its support surface. The robot moves down until it reaches the surface of the object constituting a *reach* phase. The increase in force due to contact triggers the push action to form a *push* phase.

The robot manipulator is able to squeeze and push most of the considered objects, however, the configuration fails to handle the heavy objects. In the case of the board, the object is wide which makes it rotate about the contact point during pushing. But, the robot is able to push the board to a desired location. However, with increase in the weight of the object, the single point contact starts to fail as it slips off the surface of the object.

This behavior is reflected in the measured force values during task execution as shown in figure 9. The velocity commands in z and y directions are reach and push velocities respectively. The negative velocity in the *reach* phase causes the robot to move down towards the object. A high force is measured when the robot touches the surface of the object. The established contact switches the action from push to translate where the push velocity is commanded in y direction.

In the case of a successful push of the objects, the force in z-axis which corresponds to force due to contact between object surface and the gripper, is linearly increasing in the *translate* phase. The force is constrained to 5N in this direction. The existence of force in z direction shows that a clamping force is applied on the top of the object. The comparatively higher force measured in y-axis is also increasing linearly and it also increases with the mass of the object. The maximum force measured with tissue and small plastic box is around 10N and with object with higher mass, the force exceeds 15N. The sheer force in the sponge attachment could be a source of measured force in both the directions.

The robot as mentioned earlier, fails to move the heavy paper bundle. After the contact is made with the object, the robot tries to push the object in the y direction. However, when the object fails to move, the gripper slips and moves away from the object. The region where the slippage occurs is marked in the figure 9. The trough in the graph at around 35 seconds can be interpreted as a shift from static friction to dynamic friction occurring due to the resistance offered to the motion by the surface of the paper bundle during the slip. The robot slightly moves down due to force in z direction after it slips off the object surface.

Figure 8: Single point configuration for different objects: a) Tissue. b) Board. c) Small box. d) Hollow cylinder. e) Paper bundle.

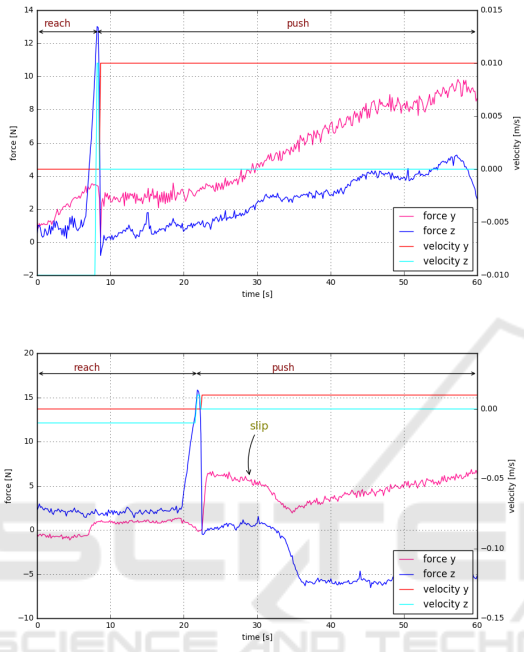

Figure 9: Force measurements from push manipulation of a set of objects with single point gripper configuration. Top: Tissue. Bottom: Paper bundle.

With the considered set of objects, the gripper configuration achieves successful push in the case of light objects irrespective of the geometry as long as it is possible to make a contact at the top surface. However, the gripper configuration does not deliver good results for a wide and/or a heavy object.

Line Configuration. A line gripper configuration provides a high surface area to establish contact with a target object, hence providing a greater grip to manipulate heavy and/or large objects. Also, the high surface area can be useful in pushing multiple small objects such as a pile of screws.

In this experiment, a heavy object, i.e., a bundle of paper is placed on a board to induce more friction in the setup. The line gripper is able to push the heavy object by aligning with a surface of the object. While the gripper can push the object when it is almost at the center of the object, pushing with a bad alignment often causes the object to rotate, eventually losing the contact with the object. In this case, an alignment strategy is used to map the measured torque to linear velocity to align the gripper with the surface of the object. The gripper is able to push the object, even when the mass is increased by adding an another bundle of paper.

In the graphs shown in figure 10, commanded velocities and the measured torque provide an overview of the experiment with two paper bundles. In the *reach* phase, the commanded velocity is in z axis to move the robot towards the object in the downward direction. The robot touches the support surface at around 20 seconds which causes peak in the torque values. The next defined action *translate* is hence triggered, causing the robot to move towards the object while in contact with the support surface. The commanded velocity in y direction is used for this action. The translation is ended when the robot touches the object, which causes the torque value to increase further. The velocity in x which corresponds alignment velocity along the surface of the object. The gripper aligns and pushes the object in *push* phase and finally *disconnects* by moving up when desired location is reached. A similar behavior was observed with reduced mass of the single paper bundle. The line gripper can easily handle the target objects when a full surface-to-surface contact is established and can serve the purpose of the design to handle heavy objects.

When line gripper is used to push objects with no even surface, for example, curved or concave objects, the design of the line gripper cannot be exploited. For instance in an experiment with a tape roll the line gripper contact is comparable to a point contact push. Although a combination of low push velocity and a good force/torque sensor can enable the line gripper to push the curved surface objects, it does not always deliver a good result.

Multi-point Configuration. A multi-point gripper is comparable to line gripper when it is aligned along a even surface of an object. It provides a contact at two points on an even surface, providing the same stability as a line gripper. The feature of the design that surpasses the design of the line gripper configuration

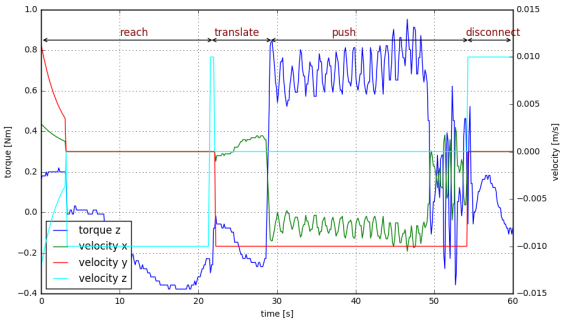

Figure 10: Commanded velocities and measured torques for push manipulation using line configuration. Two paper bundles on a board pushed using line configuration.

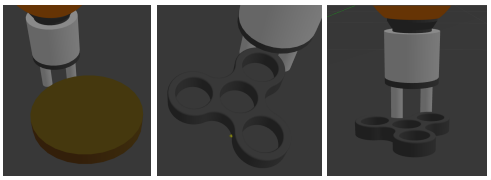

Figure 11: Multi-point configuration for different objects: a) Disc. b) Fidget spinner, convex contact surface and c) concave contact surface.

is its ability to firmly handle objects with curved and concave surfaces. A two-point gripper can be seen establishing two contacts with a disc and a fidget spinner in figure 11.

The push manipulation executed with the disc and the fidget spinner (aligning with the curve surface) in simulation and the gripper configuration was able to push both the objects to the desired location. The graphs in figure 12 show the commanded velocities and the measured torque values during execution, representing the states involved. The torque is measured by a force-torque sensor plugin in the simulation and the measurement shown in the graph is in the sensor co-ordinate system. In the *reach* phase, velocity is commanded in z-axis to move the robot in downward direction. The establishment of contact invokes the *translate* phase marked by a non-zero velocity command in y-axis.

In both cases, a single point contact is formed initially as the object is not centered with the axis of the multi-point gripper. Hence, a sudden change in the direction can be seen in the torque, and consequently in the velocity in x-axis, signifying the alignment with the surface by mapping generated torque to velocity. Further, the robot continues to push the target object in the *push* phase and finally disconnects when the target location is reached by moving up in z direction.

Although the multi-point configuration achieves the push manipulation task in this experiment, the success also depends on the distance between the two fingers of the gripper and the size of the object.

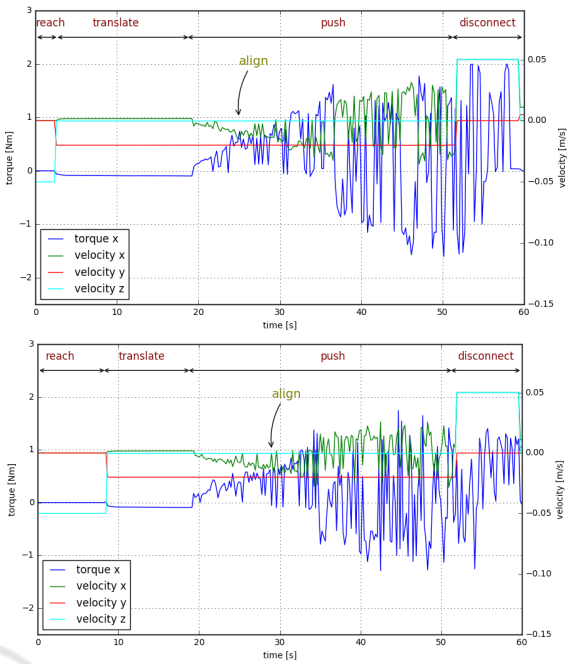

Figure 12: Commanded velocities and measured torques for push manipulation using multi-point configuration. Top: Disc. Bottom: Fidget spinner.

3.4 Control Strategies

Open Loop Control. To investigate the cases where the open loop control fails to handle the geometric properties and/or the orientations of the target objects, experiments are conducted in both simulation and real-world environment on different set of objects and push contact configurations.

We evaluate different contact situations with the line gripper and a stack of paper bundles on a cutting board: a) the line gripper is in contact near the edge of the board such that only half of the gripper surface forms contact with the board surface, b) the object stack is disoriented with respect to the gripper surface and c) the gripper makes contact with it away from the center and near the center respectively. In the first two cases, the gripper loses contact with the stack during pushing as it begins to rotate. However, in the third case, the gripper is able to keep the contact intact as the stack is only slightly rotated and hence tends to align passively with the gripper while rotating.

The experiments with open-loop control are also conducted in simulation environment with a similar and an additional case. The objects used for push manipulation are a) a slightly disoriented block (1kg) which makes an off-center contact with the gripper and b) a pile of buttons (5g each) lying away from center of the gripper. The objects are pushed using an open loop control.

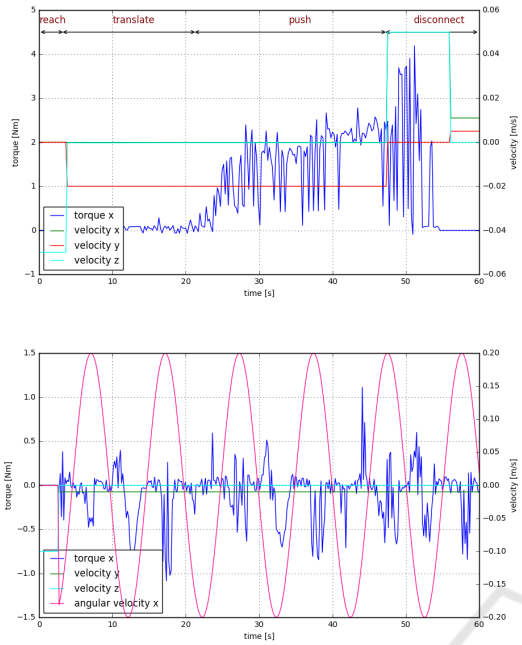

Figure 13: Commanded velocities and measured torques for different push contact configurations using open loop control. Top: Line gripper pushing at a contact away from the center of a slightly tilted block. Bottom: Line gripper induced with oscillations to handle a pile of buttons.

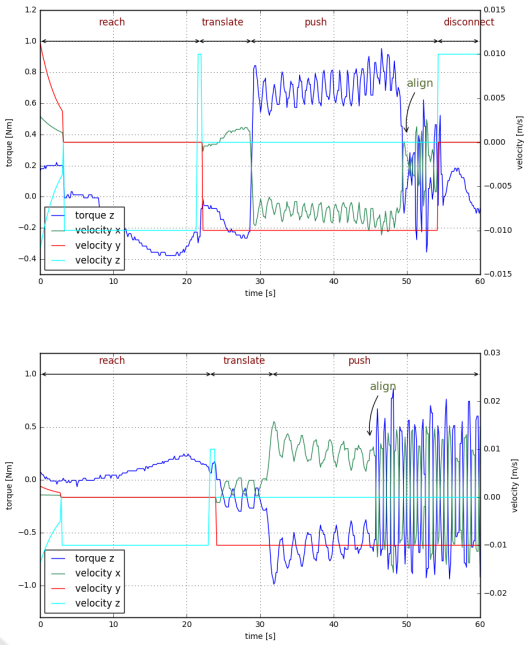

Figure 14: Commanded velocities and measured torques for different push contact configurations using closed loop control. Top: Line gripper away from the center with partial surface contact with the target object. Bottom: Line gripper away from the center with edge contact with the target object.

The velocity of -0.02m/s is commanded in y direction to push the block (a). As the object is only slightly tilted, the expected behavior would be the alignment of the gripper along the object surface as in the real world scenario. However, gazebo simulation does not handle this contact situation well, resulting in a sliding of the object along the surface of the object quickly during pushing. The measured torque values are shown in figure 13. As the *push* phase begins, the torque increases as the gripper slides away.

In the case of a pile of button, a periodic oscillation is induced in the line gripper to emulate the curved gripper design to house the multiple objects at the center of the gripper. In the graph shown in the figure 13, the angular velocity about x axis is the commanded velocity to induce oscillations given by $\omega_x = 0.2\sin(t)$. However, the objects still tend to escape away from the gripper as the gripper blindly oscillates without taking any feedback into account. In the considered case, two buttons out of three were pushed into the target location. The measured torque values capture the approximate to and fro movement of the buttons along the surface of the gripper.

Closed-loop Control. For the similar configurations of off-center contacts for the stack of paper bundles in the open loop experiment (a and b), a push manipulation is performed with a closed loop control on the real robot platform. In both cases, the gripper successfully aligns with the object surface and moves to the center while pushing the object to the target location. The resulting measurements are shown in the figure 14 for both these cases. The gripper moves along the surface and when the center is reached, the alignment is signified by oscillations. The point of this transition is vivid in both the measurements. The noise in the torque measurements in *reach* phases are due to calibration error which is fixed by online calibration before the *push* phase is entered in both cases.

The experiment on the pile of buttons is carried out in the simulation environment by mapping the torque to angular velocity instead of commanding periodic oscillations. The pile of buttons are not aligned exactly at the center in the initial push configuration. With the closed loop control the robot was able to bring the buttons to align along the surface of the gripper and push it to desired location in two out of three runs.

4 CONCLUSION

The design of simple endeffectors paired with suitable control strategies allows for the non-prehensile manipulation of a variety of objects that otherwise would be hard to grasp. We have shown that single contact endeffectors can be used to move flat, lightweight objects. Heavier objects can be successfully pushed with line-contact endeffectors. A torque-based closed-loop control strategie facilitates stable contact with the pushed objects along the trajectory without visual feedback.

REFERENCES

Al-Jarrah, O. M. and Zheng, Y. F. (1998). Intelligent compliant motion control. *IEEE Transactions on Systems, Man, and Cybernetics, Part B (Cybernetics)*, 28(1):116–122.

Alex Owen-Hill (2021). Robotics research 101: Getting started with force control. [Online].

Cosgun, A., Hermans, T., Emeli, V., and Stilman, M. (2011). Push planning for object placement on cluttered table surfaces. In *IEEE/RSJ Int. Conf. on intelligent robots and systems*.

Dogar, M. and Srinivasa, S. (2010). Push-grasping with dexterous hands: Mechanics and a method. In *IEEE/RSJ Int. Conf. on Intelligent Robots and Systems*.

Dogar, M. and Srinivasa, S. (2011). A framework for push-grasping in clutter. *Robotics: Science and systems*.

Eppner, C. and Brock, O. (2015). Planning grasp strategies that exploit environmental constraints. In *IEEE Int. Conf. on Robotics and Automation (ICRA)*.

Krivic, S. and Piater, J. (2018). Online adaptation of robot pushing control to object properties. In *IEEE/RSJ Int. Conf. on Intelligent Robots and Systems (IROS)*.

Krivic, S., Ugur, E., and Piater, J. (2016). A robust pushing skill for object delivery between obstacles. In *IEEE Int. Conf. on Automation Science and Engineering (CASE)*.

Li, Q. and Payandeh, S. (2007). Manipulation of convex objects via two-agent point-contact push. *The international journal of robotics research*, 26(4):377–403.

Lynch, K. M. (1996). *Nonprehensile robotic manipulation: Controllability and planning*. Carnegie Mellon University.

Lynch, K. M. and Murphey, T. D. (2003). Control of nonprehensile manipulation. In *Control Problems in Robotics*, pages 39–57. Springer.

Lynch, K. M. and Park, F. C. (2017). *Modern Robotics*. Cambridge University Press.

Omrčen, D., Böge, C., Asfour, T., Ude, A., and Dillmann, R. (2009). Autonomous acquisition of pushing actions to support object grasping with a humanoid robot. In *IEEE-RAS Int. Conf. on Humanoid Robots*.

Ott, C., Mukherjee, R., and Nakamura, Y. (2010). Unified impedance and admittance control. In *IEEE Int. Conf. on robotics and automation*.

Ruggiero, F., Lippiello, V., and Siciliano, B. (2018). Nonprehensile dynamic manipulation: A survey. *IEEE Robotics and Automation Letters*, 3(3):1711–1718.

Ryu, J.-C., Ruggiero, F., and Lynch, K. M. (2013). Control of nonprehensile rolling manipulation: Balancing a disk on a disk. *IEEE Transactions on Robotics*, 29(5):1152–1161.

Sarantopoulos, I. and Doulgeri, Z. (2018). Human-inspired robotic grasping of flat objects. *Robotics and autonomous systems*, 108:179–191.

Schindlbeck, C. and Haddadin, S. (2015). Unified passivity-based cartesian force/impedance control for rigid and flexible joint robots via task-energy tanks. In *IEEE Int. Conf. on robotics and automation (ICRA)*.

Serra, D. (2016). Robot control for nonprehensile dynamic manipulation tasks. In *Int. Conf. on Informatics in Control, Automation and Robotics*.

Siciliano, B., Villani, L., and Federico, N. (2000). From indirect to direct force control: A roadmap for enhanced industrial robots. *Robótica*.

Song, C. and Boularias, A. (2020). Learning to slide unknown objects with differentiable physics simulations. *arXiv preprint arXiv:2005.05456*.

Stüber, J., Kopicki, M., and Zito, C. (2018). Feature-based transfer learning for robotic push manipulation. In *IEEE Int. Conf. on Robotics and Automation (ICRA)*.

Stüber, J., Zito, C., and Stolkin, R. (2022). Let's push things forward: A survey on robot pushing. *Frontiers in Robotics and AI*, 7.

Vukcevic, D. (2020). Lazy robot control by relaxation of motion and force constraints. Technical report, Fachbereich Informatik.

Yu, K.-T., Bauza, M., Fazeli, N., and Rodriguez, A. (2016). More than a million ways to be pushed. a high-fidelity experimental dataset of planar pushing. In *IEEE/RSJ Int. Conf. on intelligent robots and systems (IROS)*.

Zeng, A., Song, S., Welker, S., Lee, J., Rodriguez, A., and Funkhouser, T. (2018). Learning synergies between pushing and grasping with self-supervised deep reinforcement learning. In *IEEE/RSJ Int. Conf. on Intelligent Robots and Systems (IROS)*.

Zhou, J., Paolini, R., Bagnell, J. A., and Mason, M. T. (2016). A convex polynomial force-motion model for planar sliding: Identification and application. In *IEEE Int. Conf. on Robotics and Automation (ICRA)*.

Zito, C., Stolkin, R., Kopicki, M., and Wyatt, J. L. (2012). Two-level RRT planning for robotic push manipulation. In *IEEE/RSJ Int. Conf. on intelligent robots and systems (IROS)*.